

On Nonlinear Combustion Instability in Liquid Propellant Rocket Motors

Gary A. Flandro* and Joseph Majdalani†

University of Tennessee Space Institute, Tullahoma, TN 37388

and

Joseph D. Sims‡

NASA Marshall Space Flight Center, Huntsville, AL 35806

*Change
Motor to engine!*

All liquid propellant rocket instability calculations in current use have limited value in the predictive sense and serve mainly as a correlating framework for the available data sets. The well-known n - τ model first introduced by Crocco and Cheng in 1956¹ is still used as the primary analytical tool of this type. A multitude of attempts to establish practical analytical methods have achieved only limited success.²⁻⁷ These methods usually produce only stability boundary maps that are of little use in making critical design decisions in new motor development programs. Recent progress in understanding the mechanisms of combustion instability in solid propellant rockets⁸⁻¹¹ provides a firm foundation for a new approach to prediction, diagnosis, and correction of the closely related problems in liquid motor instability. For predictive tools to be useful in the motor design process, they must have the capability to accurately determine: 1) time evolution of the pressure oscillations and limit amplitude, 2) critical triggering pulse amplitude, and 3) unsteady heat transfer rates at injector surfaces and chamber walls. The method described in this paper relates these critical motor characteristics directly to system design parameters. Inclusion of mechanisms such as wave steepening, vorticity production and transport, and unsteady detonation wave phenomena greatly enhance the representation of key features of motor chamber oscillatory behavior. The basic theoretical model is described and preliminary computations are compared to experimental data. A plan to develop the new predictive method into a comprehensive analysis tool is also described.

Nomenclature

\bar{a}	Mean speed of sound
e	Oscillatory energy density
\bar{E}	Time-averaged oscillatory system energy
E_m^2	Normalization constant for mode m
k_m	Wave number for axial mode m

L	Chamber length
m	Mode number
\bar{M}	Reference Mach number in chamber
n	Outward pointing unit normal vector
p	Oscillatory Pressure
\bar{P}	Mean chamber pressure
r	Radial position
R	Chamber radius
S	Strouhal Number,
t	Time
u	Oscillatory velocity vector
U_r, U_z	Mean flow velocity component
z	Axial position

*Boling Chair Professor of Advanced Propulsion, Mechanical and Aerospace Engineering. Associate Fellow, AIAA.

†Jack D. Whitfield Professor of High-Speed Flow, Mechanical and Aerospace Engineering. Member AIAA.

‡ Engineer, Combustion Devices Group, NASA Marshall Space Flight Center. Member AIAA.

Copyright © 2004 by G. Flandro, J. Sims and J. Majdalani.
Published by the American Institute of Aeronautics and Astronautics, Inc., with permission.

Greek

α	Growth rate (dimensional, sec ⁻¹)
γ	Ratio of specific heats

δ	Inverse square root of the acoustic Reynolds number, $\sqrt{\nu / a_0 R}$
ε	Wave amplitude
ν	Kinematic viscosity, μ / ρ
ρ	Density
ω	Unsteady vorticity amplitude
Ω	Mean vorticity amplitude

Subscripts

b	Combustion zone
m	Mode number

Superscripts

*	Dimensional quantity
\sim	Vortical (rotational) part
\wedge	Acoustic (irrotational) part
$(r), (i)$	Real and imaginary parts

I. Introduction

THE combustion instability problem is staggeringly complex. It involves many physical and chemical mechanisms that are not yet fully understood. This has resulted in a motor design process that, for the most part, simply ignores the possibility of combustion instability until it appears unexpectedly at the testing stage of a new system. Unfortunately, it is expensive and time consuming to correct oscillatory behavior when it is encountered in this way. Although there does exist a set of proven corrective procedures, they must still be applied in an ad hoc fashion, and without full understanding of the physical mechanisms involved. In other words, it is still a "cut-and-try" process that has evolved from difficulties such as those experienced in Saturn V (F-1) motor development.¹² In the present environment, such an occurrence would doubtless spell the cancellation of a new motor development program. In short, the ability to anticipate combustion instability problems at the design stage does not presently exist in practical form.

Nevertheless, when the findings of many investigators collected over a period of several decades are carefully merged, a comprehensive picture of the combustion instability phenomenon emerges. It is now clear that useful design tools can be devised that incorporate the seemingly divergent information that has resulted from these research programs. This has been recently demonstrated in similar problems encountered in solid propellant rocket development.^{11,13,14} The purpose of this paper is to describe methods for building this information into a new analytical model for predicting, diagnosing, and correcting problems of combustion instability in liquid propellant motors.

For any such tool to be of practical use, it must address many key design-related aspects of combustion instability. Maps of stability boundaries or linear growth rates are of very limited use in this regard. The motor design team must have powerful tools that relate possible pressure oscillation limit amplitudes, triggering pressures, and heat transfer rates to design features and motor configuration. With these tools, design tradeoffs can be accomplished to minimize the possibility of later stability problems. These analytical tools can also provide potential cost, system weight, and development time benefits, since they avoid the usual blind application of the usual acoustic baffles, resonator cavities, liners and the like that are often included without full justification or functional understanding.

In this paper we describe in detail the required physical models and their implementation. Examples are presented demonstrating the capability to represent the key elements of the combustion instability phenomenon. These include:

- Steep-fronted, shocked pressure waves
- Effects of rotational flow corrections
- Comprehensive combustion coupling including detonation wave phenomena
- Surface effects including heat transfer computations

Construction of a practical predictive analytical tool for liquid rocket ~~motor~~ combustion oscillations greatly benefits from experience with parallel developments in the solid motor arena. This experience is used to full advantage in what follows.

II. Analytical Foundations

EARLIER analyses were for the most part built upon the assumption of a system of irrotational acoustic waves. Experimental data will be reviewed showing the limitations imposed by this approach. Careless application of simplifying assumptions often leads to incorrect or incomplete results. The acoustic wave assumption is motivated by the observation that observed oscillatory frequencies are often quite close to those corresponding to the acoustic modes of the combustion chamber. However, assuming an acoustic basis for an instability theory results in the inability to accommodate correct boundary conditions (such as the no-slip condition at chamber boundaries) and the loss of important flow features such as unsteady vorticity that can have major impact on the validity of the results. It is also difficult to properly treat finite amplitude waves using an acoustic model. There is much evidence that the high-amplitude wave systems in unstable rockets are more akin to traveling shock fronts.¹⁵⁻¹⁸ Early efforts

were made to account for steepened wave effects⁶⁻⁷, but the analytical methods applied did not lead to practical solutions. These were usually applications of the method of characteristics that did not lend themselves well to generalized computational techniques of the kind needed for a practical stability assessment algorithm.

Experience with Solid Propellant Motors

The well-known failure of predictive algorithms in solid rocket analysis is largely the result of neglect of key features of the unsteady flow of combustion products. In particular, one must account for effects of vorticity production and propagation and for the tendency of initially weak (essentially acoustic) waves to steepen into shock-like wave motions. When such waves interact with a combustible mixture of injectants, then the possibility of unsteady detonation waves must also be addressed. Very significant improvement in predictive capability results from inclusion of these features, which until recently were not included in either liquid or solid motor analyses

Solid propellant rocket motor analysis as applied in the SSP (Standard Stability Prediction) computer program, implements Culick's irrotational acoustics based analyses.^{2-4,8-11,19-23} While the Culick approach introduces a more complete formulation than similar algorithms in the accepted liquid rocket tool kit, it does not yield satisfactory predictive capability. This is partly the result of the assumption that the wave motions are strictly acoustic (irrotational) in nature. Recent work by the writers of the present paper focused on improving SSP by inclusion of important mechanisms such as vorticity generation and shock wave interactions. Much of the recent progress in the solid motor analysis leads directly to similar improvements in handling the liquid rocket instability problem.

Culick's papers on combustion instability^{20,21,24-26} published in the early 1970's are the foundation for all stability prediction methods now in use.^{27,28} His method is based on three crucial assumptions:

- small amplitude pressure fluctuations superimposed on a low-speed mean flow,
- thin, chemically reacting surface layer with mass addition, and
- oscillatory flow-field represented by chamber acoustic modes.

The first assumption allows linearization of the governing equations both in the wave amplitude and the surface Mach number of the mean injected flow. The second causes all surface reaction effects, including combustion, to collapse to simple acoustic admittance boundary conditions imposed at the chamber surfaces.

The last assumption oversimplifies the oscillatory gas dynamics by suppressing all unsteady rotational flow effects; the acoustic representation is strictly irrotational. Concern for this omission was addressed partially by Culick in a paper in which he introduced his well-known rotational mean flow model.²⁵ Stability calculations based on this improved mean flow representation produced no significant changes in the system stability characteristics. On this basis, it has since been generally assumed that all vorticity (rotational flow effects), including the unsteady part, have negligible influence on combustion instability growth rate calculations.

Rotational Flow Effects

Considerable progress has been made in the last decade in understanding both the precise source of the vorticity and the resulting changes in the oscillatory flow-field. Analytical,^{10,29-36} numerical,³⁷⁻⁴² and experimental investigations⁴³⁻⁴⁶ have demonstrated that rotational flow effects play an important role in the unsteady gas motions in solid rocket motors. Much effort has been directed to constructing the required corrections to the acoustic model. This has culminated in a comprehensive picture of the unsteady motions that agrees with experimental measurements,^{10,29,30} as well as numerical simulations.³¹

These models were used in carrying out three-dimensional system stability calculations,^{10,29} in a first attempt to account for rotational flow effects by correcting the acoustic instability algorithm. In this process one discovers the origin, and the three-dimensional form, of the classical *flow-turning* correction; related terms appear that are not accounted for in the SSPP algorithm. In particular, a rotational correction term was identified that cancels the flow-turning energy loss in a full-length cylindrical grain. However, all of these results must now be questioned because they are founded on an incomplete representation of the system energy balance.

Culick's stability estimation procedure is based on calculating the exponential growth (or decay) of an irrotational acoustic wave; the results are equivalent to energy balance models used earlier by Cantrell and Hart.⁴⁷ In all of these calculations the system energy is represented by the classical Kirchhoff (acoustic) energy density. Consequently, it does not represent the *full* unsteady field, which must include both acoustic and rotational flow effects. Kinetic energy carried by the vorticity waves is thus ignored. It is readily demonstrated that the actual average unsteady energy contained in the system at a given time is about 25% larger than the acoustic energy alone.¹¹ Furthermore, representation of the energy sources and sinks that determine the stability characteristics of the motor chamber must also be modified. Attempts to correct

the acoustic growth rate model by retention of rotational flow source terms only,,^{10,29} preclude a full representation of the effects of vorticity generation and coupling.

In liquid motors, the main role played by the rotational flow interactions is in controlling boundary conditions at the chamber walls and especially at the injector boundaries. Vorticity is created in the case of waves traveling parallel to the injection interface because such waves (tangential modes for example) represent unsteady pressure gradients across the incoming quasi-steady flow streamlines. This vorticity is propagated into the chamber mainly by convection, and it has important implications in terms of the motor stability. These effects will be examined carefully as we carry out the stability analyses in the next section of the report.

Nonlinear Effects

The effects of nonlinear interactions play a major role in controlling all important attributes of nonlinear pressure oscillations in liquid motor combustion chambers. Thus strictly linearized models are of little value in the present situation. Of crucial importance is the modeling of the time history of the oscillations and their limiting amplitude and the critical triggering amplitudes at which an otherwise stable motor is caused to transition to violent oscillations. Pulsing of this sort can occur from random "popping" and other natural disturbances, so it is important to characterize this aspect of motor behavior.

It is well-known that shock waves are a major nonlinear attribute of axial mode oscillations in solid rockets.⁴⁸⁻⁵¹ Current work with liquid motor preburners shows similar longitudinal mode shocks.⁵² We will now establish that similar effects are associated with transverse modes despite widely-held contrary views.⁵³

Transverse Mode Shock and Detonation Waves

Study of the Saturn V first stage F-1 engine development stability problems⁵⁴ gives much guidance in the modeling requirements addressed in this paper. Examination of the oscillatory pressure data for this motor (see Fig. 1) indicate the presence of steep fronted, shock-like waves.

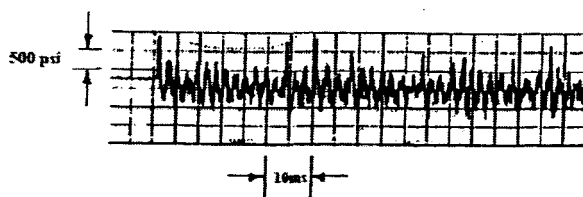


Fig. 1 Shock Waves in F-1 Pressure Trace.^{12,54}

This is such a familiar case, that we will not give a detailed account here. Instead, we emphasize related information that was apparently ignored by the combustion instability research community. In particular, we focus in this subsection on the strong evidence for shock and detonation wave effects as an integral feature of liquid rocket instability. In the course of the F-1 investigation basic research was conducted in the late 1960's at the Caltech Jet Propulsion Laboratory by Clayton and his co-workers using a highly instrumented liquid rocket motor illustrated in Fig. 2.^{15-18,55}

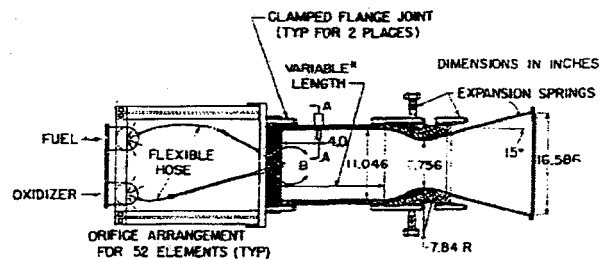


Fig. 2 JPL 20k-lbf-Thrust Rocket Motor.¹⁸

This device allowed detailed measurement not only of the unsteady pressure waves throughout the motor cavity, but also included motion-picture recording of events within the chamber by means of a protected camera placed just outside nozzle throat (sans exit cone).^{16,55} The investigators described the unsteady flow field as a "traveling detonation wave." The presence of steep high-amplitude wave fronts is clearly depicted in the pressure traces measured near the injector face as shown in Fig. 3.

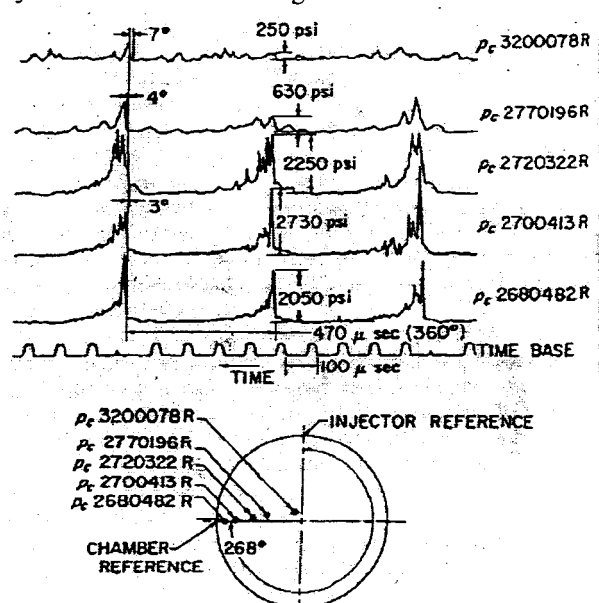


Fig. 3 Evidence of Shock Waves in JPL 20k-lbf-Thrust Rocket Motor.¹⁸

The waves were identified by their dominant frequency component as the first tangential acoustic mode. This mode is often associated with the most destructive forms of liquid rocket instability. Although the waveform is steep fronted, it is basically a "shocked" acoustic wave of very large amplitude (on the acoustic scale). Figure 4 shows how the wave energy is distributed axially in the motor. This data was secured using an ablatively cooled Kistler pressure probe that could be accurately placed laterally and axially within the motor chamber. Notice that the kinetic energy associated with the wave is strongest near the chamber wall and is barely discernible in the nozzle entrance. This provides direct verification of modeling assumptions routinely used in handling the unsteady nozzle boundary conditions. The records were obtained during resonant combustion initiated by a 25 msec bomb pulse.

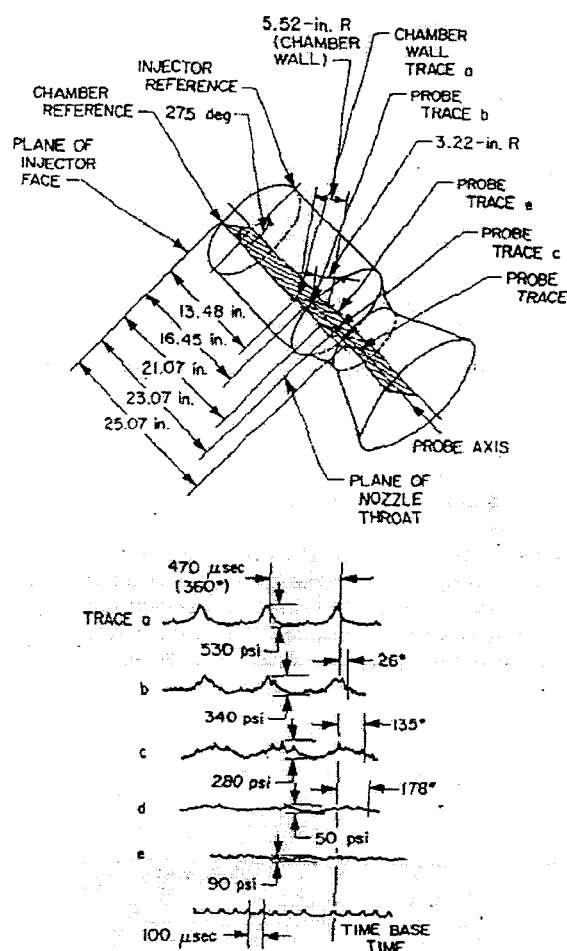


Fig. 4 Axial Distribution of Wave Amplitude in JPL 20k-lbf-Thrust Rocket Motor.¹⁸

III. Formulation

IN this section we briefly discuss what is needed from the theoretical standpoint to provide a useful analytical framework for combustion instability. It is necessary to accommodate the features we have identified as key elements in a correct physical representation. We must discard models based on the acoustic point of view. Nonlinear energy losses in steep wave fronts and energy flow to the wave structure from combustion must be accommodated. It is also necessary to provide a framework that can ultimately include effects of mixing, vaporization, and other two phase flow effects. These elements will be included only in outline form, but placeholders are inserted which will require later elaboration. The most effective method for incorporating this large array of physical/chemical interactions is by using a global nonlinear energy balance. Methods based on the usual perturbed acoustic wave equation cannot properly account for the many interactions that must be included.

Mathematical Strategy

Since a central concern is the handling of steep fronted waves it is necessary to carefully lay out a solution technique that will lead to a practical predictive algorithm. To make the mathematical problem tractable, we choose to avoid the fashionable numerical strategies such as method of characteristics of a full CFD treatment of the problem. Either of these techniques would likely fail in the problem we are attempting to solve here. What is required is an approach that bridges the gap between the earlier perturbation techniques that limit the solutions to linear gas motions and other ad hoc methods such as those introduced by Culick to study nonlinear features of combustion instability.^{22,56,57} In those works, Culick and his students model the steepening process in which energy flows by nonlinear mode coupling from low frequency to higher frequency spectral components.

In the problem of central interest here, we are not concerned with the steepening process, per se, rather, we wish to understand the gas motions in the fully steepened state. Figure 5 illustrates several aspects of the problem we must solve. This diagram shows in schematic form all features of combustion instability that appear experimentally. Furthermore, it provides a useful way to categorize the various analytical methods by which we attempt to understand this very complicated physical problem. Figure 5 shows that if the waves grow from noise in the linear fashion, the motion is linear and each acoustic mode grows individually according to the balance of energy gains and losses peculiar to that operating frequency. In general, the lowest order mode grows most rapidly because it requires less energy to excite. As the oscillations grow to a finite amplitude, nonlinear effects appear and there

is a phase in which energy is redistributed from lower to higher modal components; it is this process that is described in Culick's nonlinear model.

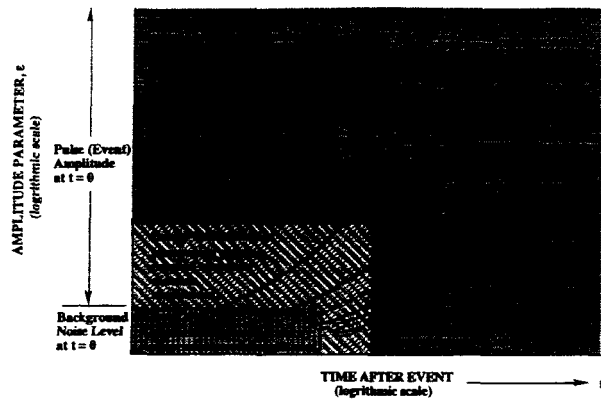


Fig. 5 Time Evolution of System Amplitude

As the wave steepens, the relative amplitudes of the constituent acoustic modes reach a frozen state corresponding to shock like behavior. This is the fully nonlinear state illustrated in the figure. In pulse testing of motors, the steepening process is almost instantaneous. For example, Brownlee⁴⁸ notes that when the pulse is fired, "...the injected flow disturbance traversed the length of the motor, partially reflected at the nozzle end, and became a steep-fronted shock-like wave in one cycle." Thus in modeling such effects, it is unnecessary to trace the full steepening process. The relative wave amplitudes are readily estimated from a large database of experimental data to be described later. It is readily established that precise knowledge of the relative amplitudes is not necessary to achieve an accurate estimate of the limit cycle and triggering amplitudes.

We must formulate a mathematical strategy that yields the key information, namely the limit amplitude reached by the system in the fully steepened state. This is the information required by the motor designer in assessing potential vibration levels, and as we will show, the severity of heat loads and force levels on fragile injector components.

The key to simplifying the nonlinear problem is to assume that the fully steepened traveling wave is a composite of the chamber normal modes:

$$p(r, t) = \varepsilon(t) \sum_{m=1}^{\infty} A_m(t) \psi_m(r) \quad (1)$$

where $\varepsilon(t)$ is the instantaneous amplitude. This is a proven simplifying strategy^{49,50} that conforms well to all experimental features that must be accommodated in our solution algorithm.

Notation

The following dimensionless variables will be used (star * denotes dimensional quantities; subscript o indicates quiescent chamber reference conditions):

$$\begin{cases} p = p^*/P_o \\ \rho = \rho^*/\rho_o \\ T = T^*/T_o \\ u = u^*/a_o \\ r = r^*/L \end{cases} \quad \begin{cases} F = F^*/(\rho_o a_o^2/L) \\ t = t^*/(L/a_o) \\ \omega = \omega^*/(a_o/L) \\ e = e^*/a_o^2 \end{cases} \quad (2)$$

where F is a body force and e is specific internal energy. The dimensionless governing equations are:

Continuity:

$$\frac{\partial \rho}{\partial t} + \nabla \cdot (\rho u) = 0 \quad (3)$$

Momentum:

$$\begin{aligned} \rho \left(\frac{\partial u}{\partial t} + \frac{1}{2} \nabla u \cdot u - u \times \omega \right) = \\ = -\frac{1}{\gamma} \nabla p - \delta^2 \nabla \times \nabla \times u + \delta_a^2 \nabla (\nabla \cdot u) + F \end{aligned} \quad (4)$$

Energy:

$$\begin{aligned} \frac{\partial}{\partial t} \left[\rho \left(e + \frac{1}{2} u \cdot u \right) \right] + \nabla \cdot \left[\rho u \left(e + \frac{1}{2} u \cdot u \right) \right] = \\ = \left\{ \begin{aligned} & \frac{\delta^2}{(\gamma-1)Pr} \nabla^2 T - \frac{1}{\gamma} \nabla \cdot (p u) + \rho u \cdot (u \times \omega) \\ & + u \cdot F + \delta^2 [\omega \cdot \omega - u \cdot \nabla \times \omega] + \\ & + \delta_a^2 [(\nabla \cdot u)^2 + u \cdot \nabla (\nabla \cdot u)] - \sum_{i=1}^N h_i^0 w_i \end{aligned} \right\} \quad (5)$$

Species mass fraction:

$$\rho \left[\frac{\partial Y_i}{\partial t} + u \cdot \nabla Y_i \right] - \frac{\delta^2}{Pr} \nabla^2 Y_i = w_i \quad (6)$$

State:

$$p = \rho T \quad (7)$$

The Prandtl number Pr and viscous reference lengths (proportional to inverse square root of appropriate Reynolds numbers) appear naturally. These are defined as:

$$\begin{cases} Pr \equiv \frac{c_p \mu}{\kappa} \\ \delta^2 = \frac{\nu}{a_o L} \\ \delta_a^2 = \delta^2 \left(\eta / \mu + \frac{4}{3} \right) \\ \delta_f \equiv \frac{\kappa}{\rho_o c_p V_{ref}} = \frac{\kappa}{\rho_o c_p a_o M_{ref}} \end{cases} \quad (8)$$

The latter reference length is the reference flame length needed in regions dominated by combustion heat

release. Other variables needed in modeling chemical reactions are:

$$\begin{cases} w = w^*/(\rho_0 a_0/L) = \\ \quad \text{= Dimensionless reaction rate} \\ h_i^o = (h_i^o)^*/a_0^2 = \\ \quad \text{= Dimensionless heat of combustion} \\ Y_i = \text{Mass fraction for species } i \end{cases} \quad (9)$$

Decomposing Variables: Steady and Unsteady Parts

The steady and unsteady parts of the variables are separated in the standard manner by writing

$$\begin{cases} \rho = \bar{\rho} + \rho^{(i)} \\ p = \bar{p} + p^{(i)} \\ T = \bar{T} + T^{(i)} \\ \mathbf{u} = \bar{\mathbf{M}}_b \mathbf{U} + \mathbf{u}^{(i)} \\ \boldsymbol{\omega} = \bar{\mathbf{M}}_b \nabla \times \mathbf{U} + \nabla \times \mathbf{u}^{(i)} = \bar{\mathbf{M}}_b \boldsymbol{\Omega} + \boldsymbol{\omega}^{(i)} \end{cases} \quad (10)$$

Since the energy balance is the key to understanding the system behavior, let us carefully work with it. In what follows, we will avoid the common simplifying assumptions such as the isentropic flow limitation. We will also carefully include heat transfer and viscosity so that, in effect, we are modeling a wave system composed of superimposed waves of compressibility, vorticity, and entropy.

Define the system energy density as

$$\mathcal{E} \equiv \rho \left(e + \frac{1}{2} \mathbf{u} \cdot \mathbf{u} \right) \quad (11)$$

Then for a calorically perfect gas the energy equation becomes

$$\begin{aligned} \frac{\partial \mathcal{E}}{\partial t} = & -\nabla \cdot \left[\rho \mathbf{u} \left(\frac{T}{\gamma(\gamma-1)} + \frac{1}{2} \mathbf{u} \cdot \mathbf{u} \right) \right] + \\ & \left\{ -\frac{1}{\gamma} \nabla \cdot (p \mathbf{u}) + \rho \mathbf{u} \cdot (\mathbf{u} \times \boldsymbol{\omega}) + \right. \\ & + \delta^2 [\boldsymbol{\omega} \cdot \boldsymbol{\omega} - \mathbf{u} \cdot \nabla \times \boldsymbol{\omega}] + \frac{\delta^2}{(\gamma-1)P_r} \nabla^2 T + \\ & \left. + \delta_d^2 [(\nabla \cdot \mathbf{u})^2 + \mathbf{u} \cdot \nabla (\nabla \cdot \mathbf{u})] + \dot{Q} + \mathbf{u} \cdot \mathbf{F} \right\} \end{aligned} \quad (12)$$

where a shorthand notation has been adopted for the heat release in the combustion processes. The body force, \mathbf{F} , is a placeholder for several two-phase flow effects such as spray atomization, etc. that will be treated later. Note that the dilatational viscous force and conduction heat transfer terms are retained. These are the source of the important nonlinear energy loss in steep wave fronts.

Using Eqs. (10), one can now expand Eq. (11) to give the equation for the system amplitude. To accomplish this, the time averaged Eq. (12) can be written as

$$2\epsilon \frac{d\epsilon}{dt} \langle E_2 \rangle = \left\langle \begin{aligned} & -\nabla \cdot \left[\rho \mathbf{u} \left(\frac{T}{\gamma(\gamma-1)} + \frac{1}{2} \mathbf{u} \cdot \mathbf{u} \right) \right] - \\ & -\frac{1}{\gamma} \nabla \cdot (p \mathbf{u}) + \rho \mathbf{u} \cdot (\mathbf{u} \times \boldsymbol{\omega}) + \mathbf{u} \cdot \mathbf{F} + \dot{Q} \\ & + \delta^2 [\boldsymbol{\omega} \cdot \boldsymbol{\omega} - \mathbf{u} \cdot \nabla \times \boldsymbol{\omega}] + \delta_d^2 \mathbf{u} \cdot \nabla (\nabla \cdot \mathbf{u}) + \\ & + \left\{ \frac{\delta^2}{(\gamma-1)P_r} \nabla^2 T + \delta_d^2 (\nabla \cdot \mathbf{u})^2 \right\} \end{aligned} \right\rangle \quad (13)$$

where

$$\langle E_2 \rangle = \frac{1}{\gamma \bar{P}} \left\langle \left(\frac{p'}{\gamma} \right)^2 \right\rangle + \frac{1}{2} \bar{\rho} \langle \mathbf{u}' \cdot \mathbf{u}' \rangle \quad (14)$$

is the time averaged oscillatory energy. Note that this consists of a "potential" energy proportional to the pressure fluctuation and a kinetic part proportional to the square of the particle velocity. The latter is not the simple acoustic particle velocity; it is the composite of the irrotational and rotational parts needed to satisfy correct boundary conditions at the chamber surfaces.

Equation (14) is similar to the usual Kirchhoff reference energy density from classical acoustics⁵⁸:

$$\mathcal{E}_{\text{Kirchoff}} = \frac{1}{2} \left(\frac{p^{(i)}}{\gamma} \right)^2 + \frac{1}{2} \bar{\rho} \mathbf{u}^{(i)} \cdot \mathbf{u}^{(i)} \quad (15)$$

The differences are largely the result of relaxing the isentropic flow assumption used in deriving Eq. (15).

Spatial Averaging

In order to account for the net behavior of the entire system it is now required to integrate the time-averaged energy density over the chamber control volume. Define the reference system energy,

$$\begin{aligned} E^2 & \equiv \iiint_V \langle \mathcal{E}_2 \rangle dV = \\ & = \iiint_V \left\langle \frac{1}{\gamma \bar{P}} \left(\frac{p'}{\gamma} \right)^2 + \frac{1}{2} \bar{\rho} \mathbf{u}' \cdot \mathbf{u}' \right\rangle dV \end{aligned} \quad (16)$$

Then the rate of change of system amplitude can be written in the convenient form:

$$\frac{d\epsilon}{dt} = \alpha^{(1)} \epsilon + \alpha^{(2)} \epsilon^2 + \alpha^{(3)} \epsilon^3 + \dots \quad (17)$$

where $\alpha^{(i)}$ is the linear growth rate for the composite wave system. This expression emphasizes the important fact that the nonlinear model is only as good as the linear representation of the system.

In many ways, achieving a valid linear model is the most difficult part of the entire problem. It has in fact been the downfall of numerous past attempts. Much time and energy has been expended on attempts to correct deficiencies in the linear model by introduction of ad hoc fixes that are often based on guesswork, and misinterpretation and/or distortion of experimental evidence. The roadway is strewn with the wreckage of such attempts. We avoid the temptation to dwell on this unhappy aspect of the past. Clearly, the only road to success is to avoid losing any of the crucial physical information that have been so carefully collected in the system energy balance constructed here.

Linear Growth Rate

The linear part of Eq. (17) becomes

$$\alpha^{(1)} = \frac{1}{2E^2} \left\{ \begin{aligned} & -\frac{1}{\gamma} \iint_S \mathbf{n} \cdot \langle \mathbf{p}' \mathbf{u}' \rangle dS - \\ & -\frac{\bar{M}_b}{\gamma \bar{P}} \iint_S \mathbf{n} \cdot \mathbf{U} \left\langle \left(\frac{p'}{\gamma} \right)^2 \right\rangle dS - \\ & -\bar{M}_b \bar{P} \iint_S \mathbf{n} \cdot \left\langle \frac{1}{2} \mathbf{U} (\mathbf{u}' \cdot \mathbf{u}') + \mathbf{u}' (\mathbf{U} \cdot \mathbf{u}') \right\rangle dS + \\ & +\bar{M}_b \bar{P} \iiint_V \langle \mathbf{u}' \cdot (\mathbf{u}' \times \boldsymbol{\Omega}) \rangle dV + \\ & +\bar{M}_b \bar{P} \iiint_V \mathbf{U} \cdot \langle \mathbf{u}' \times \boldsymbol{\omega}' \rangle dV + \\ & +\bar{M}_b \bar{P} \iiint_V \langle \mathbf{u}' \cdot (\mathbf{U} \times \boldsymbol{\omega}') \rangle dV + \\ & +\delta^2 \iint_S \mathbf{n} \cdot \langle \mathbf{u}' \times \boldsymbol{\omega}' \rangle dS + \\ & +\delta_a^2 \iiint_V \langle \mathbf{u}' \cdot \nabla (\nabla \cdot \mathbf{u}') \rangle dV + \\ & +\iiint_V \langle \dot{Q} \rangle dV + \iiint_V \langle F \rangle dV \end{aligned} \right\} \quad (18)$$

where only the placeholders for combustion heat release and two-phase flow interactions are shown. It happens that careful evaluation of the volume integrals in Eq. (18) leads to vanishing many of the terms shown. One of these is the Culick flow turning effect, which has been the source of considerable argument, disagreement, and unhappiness in the solid propellant rocket instability research community. Unfortunately, this term leads to a damping effect which in most motor evaluations is as large as other main contributions to the energy balance. To illustrate the handling of terms in Eq. (18), we now (correctly) evaluate the term from which flow turning originates:

$$\alpha_4^{(1)} = \frac{\bar{M}_b \bar{P}}{2E^2} \iiint_V \left(\mathbf{U} \cdot \langle \mathbf{u}' \times \boldsymbol{\omega}' \rangle + \langle \mathbf{u}' \cdot \mathbf{U} \times \boldsymbol{\omega}' \rangle \right) dV \quad (19)$$

The subscript, 4, is an artifact of the numbering system introduced in Ref. (11) to keep track of the many linear stability contributions in Eq. (18). Flow turning was first identified by Culick^{21,26} in his one-dimensional calculations as a result of forcing satisfaction the no-slip condition (which could not be accomplished in his three-dimensional model because of the irrotational flow assumption). Flandro^{10,11,29,59} later showed that the actual source of the flow turning was the irrotational part of the second term in Eq. (19). None of the earlier stability calculations incorporated all of the rotational terms included in Eq. (19). When *all* of the terms are properly accounted for, it is readily seen by applying the standard scalar triple product identity

$$\mathbf{A} \cdot (\mathbf{B} \times \mathbf{C}) = \mathbf{B} \cdot (\mathbf{C} \times \mathbf{A})$$

that:

$$\begin{aligned} \mathbf{U} \cdot \langle \mathbf{u}' \times \boldsymbol{\omega}' \rangle + \langle \mathbf{u}' \cdot \mathbf{U} \times \boldsymbol{\omega}' \rangle &= \\ = \langle -\mathbf{u}' \cdot \mathbf{U} \times \boldsymbol{\omega}' \rangle + \langle \mathbf{u}' \cdot \mathbf{U} \times \boldsymbol{\omega}' \rangle &= 0 \end{aligned} \quad (20)$$

Flow turning has now vanished; a result that agrees with several other studies.^{60,61}

This correction alone leads to major improvement in agreement with experimental data. The lesson here is that only by accounting for *all* unsteady energy gains and losses can a correct linear stability theory be achieved. Other terms in Eq. (18) once thought to have important stability implications do not appear when the integrals are carefully evaluated.

We have recently completed a full evaluation of Eq. (18) for the solid motor case; current efforts are focused on a similar evaluation for the liquid motor case. This has already been done for longitudinal waves (initial results are described in a companion paper⁵²); major effort is now being devoted to the important transverse mode case of central importance in large motor development programs.

Effects of Nonlinearity

It is now required to examine nonlinear terms arising from the expansion of Eq. (13). The most important of these are the energy losses incurred in steep wave fronts. Let us focus on the last set of terms in Eq. (13). After temporal and spatial averaging, we are left with

$$\iiint_V \left\langle \frac{\delta^2}{(\gamma-1)P_r} \nabla^2 T + \delta_a^2 (\nabla \cdot \mathbf{u})^2 \right\rangle dV \quad (21)$$

Those readers experienced in gasdynamics will recognize in this term the source of the entropy gain and associated energy loss in a steep wave front. In fact, this term is usually ignored because it is only important if there are very steep gradients in particle velocity and temperature. Let us evaluate this term by considering a very small portion of the chamber volume that encompasses the shock layer formed by a steepened wave system as described earlier. The shock

layer can be treated as a region of nonuniformity as illustrated in Fig. 6.

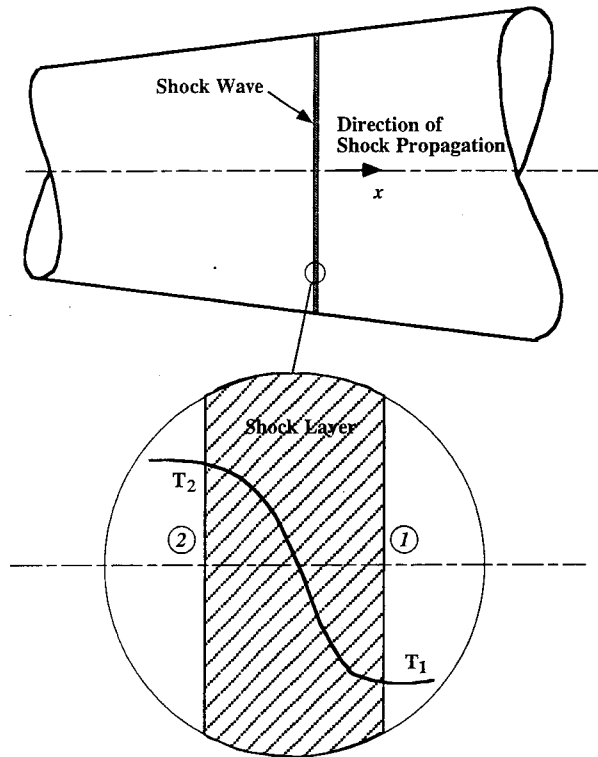


Fig 6 Shock Layer Structure

Following standard procedures Eq. (21) can be reduced to the classical textbook result showing the origin of the entropy gain in the shockwave. By manipulations using the Rankine-Hugoniot equations, we find the formula for the energy loss in the steep wave to be

$$\left(\frac{dE}{dt}\right)_{\text{shock}} = -\frac{S_{\text{port}}}{\gamma(\gamma-1)} \frac{(s_2 - s_1)^*}{c_v} = -\left(\frac{\epsilon_{\text{shock}}}{P}\right)^3 S_{\text{port}} \left(\frac{\gamma+1}{12\gamma^3}\right) \quad (22)$$

leading to a simple approximation for the nonlinear stability parameter in Eq. (17), namely

$$\alpha^{(2)} = -\frac{(\gamma+1)}{3E^2} \left(\frac{\xi}{2\gamma}\right)^3 S_{\text{port}} \quad (23)$$

where ξ is a factor dependent upon the assumed waveform for the traveling shock wave, and S_{port} is the area of the shock front. In the longitudinal case, this is simply the cross-sectional area of the duct at a convenient location.

This nonlinear loss effect is the principal damping mechanism in both liquid and solid propellant motors, and is the key element in understanding the limit cycle behavior so often encountered when finite amplitude

waves appear. It is tempting to carry the implied perturbation series in Eq. (17) to higher than second order in the system amplitude. However, this is not justified in the present situation because we assume that the unsteady flow field and mode shape information for the chamber is accurate only to the first order in wave amplitude. Let us now test the results that we have found against experimental evidence.

Limit Cycle Amplitude

In liquid propellant motors one is seldom interested in tracing the details of the growth of the waves to their final state. Such motors usually operate for very long time on the time scale of the wave motions with very slow changes in the steady operating parameters. For this reason, strictly linear models provide very little use information in the predictive sense. There is, however, a well-known rule of thumb that suggests that large values of the linear growth rate, $\alpha^{(1)}$, estimated for example by using Eq. (18) correlate with large values of the limit cycle amplitude. Clearly it is the latter amplitude that is of concern, since it is a measure of the vibration and other impacts on the system due to the oscillations.

What is required is information concerning the limit amplitude reached as the wave system approaches its fully steepened form. Equation (17) provides the required limit amplitude. In the fully steepened state, the wave amplitude is stationary, and it is readily seen that the limit amplitude is

$$\epsilon_{\text{limit}} = -\frac{\alpha^{(1)}}{\alpha^{(2)}} \quad (24)$$

which is physically meaningful only when $\alpha^{(2)}$ is negative. This will always be the case for the shock loss mechanism described by Eq. (23). This expression has been tested for many solid rocket data sets and has been found to yield an excellent estimate of the limit amplitude. Again, please note that good results depend critically on a valid linear stability estimate.

Triggering Amplitude

This is a controversial subject. If one examines Fig. 5, in the context of Eq. (17) with extension to higher orders in the wave amplitude, it is readily seen that it is theoretically possible to raise the amplitude of a system oscillating at its lowest limit amplitude to a yet higher limit amplitude by adding sufficient energy in a pulse to raise the oscillations above a critical triggering level as described in the figure. This is what might be termed *true triggering*. Careful examination of solid rocket data shows that this scenario seldom fits what is actually observed. In every case studied by the authors, motors that exhibited "triggering" were linearly unstable motors. That is, they are not stable motors that

are *triggered* into a high-amplitude limit cycle. When such motors operate without deliberate pulsing, the wave system grows so slowly from the random noise that is always present, that oscillations are barely measurable by the end of the burn. However, when the motor is disturbed by a sufficiently large pulse, the broadband energy increment excites finite amplitude steep fronted waves. The system then grows rapidly to the limit cycle amplitude. Calculations using Eq. (24) agree very well with actual observations. We believe that true triggering is seldom, if ever, observed in actual rocket motors. Much of the confusion over this issue has resulted from application of faulty predictive codes that almost always predict a linearly stable system. A classic example can be found in the recent experiments by Blomshield.⁶² Every motor fired in this test series was predicted by the SSP (standard stability prediction code) to be linearly stable. In fact many of the motors were linearly unstable at least during part of the burn. Unless pulsed, only very low level oscillations were present. Sufficiently strong pulsing during linearly unstable operation led to violent oscillations in several tests.

IV. Conclusions; Application to Liquid Motors

WE have recently used the model described in this paper in the analysis of longitudinal mode oscillations in liquid propellant motor preburners.⁵² Preliminary findings are reported in a companion paper. As in the case of the solid motor application, predictive capability is very promising and the results compare favorably to measurements.

In applying the results to large liquid rockets with potential transverse mode instability, considerable work remains to be accomplished. In particular, it is necessary to treat the three-dimensional coupling between the waves and the combustion heat release. The first step is to establish that steep waves can be formed in the transverse mode case. The information set forth in Part II of this paper convincingly shows that steep-fronted waves do represent an important feature of high-amplitude transverse mode liquid rocket combustion instability.

Another aspect of the problem requiring attention is the application of detonation wave physics to the combustion model in the present situation. Clearly, shock motions in the unreacted gas mixture in the injection process may have a large impact on the energy transfer from combustion to the wave system.

It remains to demonstrate that a simple model of the type used in the longitudinal case (see Eq. (1)) is valid for transverse modes. It is very important that we avoid the use of method of characteristics or full Navier-Stokes CFD algorithms in attempts to model this problem. What is needed is a simple model that can

rapidly and accurately determine the system stability characteristics without the expense and time required in a strictly numerical attack on the problem. This is not to say that there is not a future role for CFD in the solution of combustion instability problems. However, a crucial first step is to perfect a simple predictive algorithm based on concepts such as those developed in this paper.

An important step is to simplify the mathematical description of the unsteady flow field. It is possible to utilize a three-dimensional form of Eq. (1) to represent a steep fronted traveling tangential mode; Bessel function mode shapes are then required. Figure 7 is a frame from an animation of calculations describing a steep wave front formed by superimposing a set of standing tangential modes. Twenty modes were used to produce the model shown. The traveling shockwave traverses the chamber once each period of the first tangential mode. This representation of the unsteady flow is in excellent agreement with what is described in the F-1 data and in Clayton's excellent measurements.

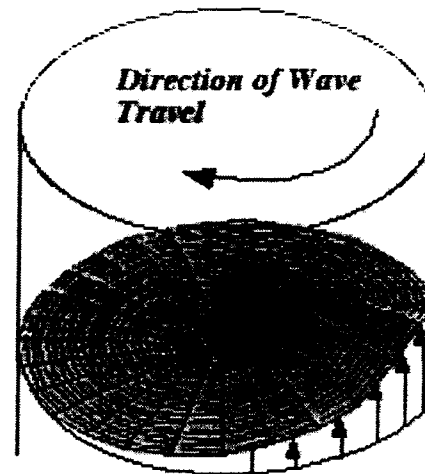


Fig 7 Simulated Traveling Tangential Shock Wave

These findings are contrary to accepted ideas, which hold that transverse modes cannot steepen even though very large amplitudes might be present. The classical work of Maslen and Moore is often cited as proof of this idea.⁵³ However, this view does not agree with much experimental data already described that indicates otherwise.

Finally, it should be observed that a high-amplitude steep wave front traveling across the injector face will have major impact on heat transfer rates and on transverse forces acting on surface structures. The authors believe that this is the mechanism that leads to severe injector damage often associated with finite amplitude combustion oscillations in motor chambers.

Acknowledgements

This work was sponsored partly by the University of Tennessee, UTSI, and partly by the NASA Marshall Spaceflight Center, under Grant No. NNM04AA30G, Technical Officer, J. D. Sims. The first author wishes to express appreciation for additional support from the Edward J. and Carolyn P. Boling Chair of Excellence in Advanced Propulsion, University of Tennessee.

References

- ¹Crococo, L., and Cheng, S. I., "Theory of Combustion Instability in Liquid Propellant Rocket Motors," *Agard*, Vol. 8, Butterworths Sci. Pub. Ltd, London, UK, 1956.
- ²Culick, F. E. C., "High Frequency Oscillations in Liquid Rockets," *AIAA Journal*, Vol. Vol. 1, No. No. 5, 1963, pp. 1097-1104.
- ³Culick, F. E. C., and Yang, V., "Overview of Combustion Instabilities in Liquid Propellant Rocket Engines," *Liquid Rocket Engine Combustion Instability*, Vol. 169, AIAA Progress in Astronautics and Aeronautics, 1995, pp. 1-37.
- ⁴Culick, F. E. C., "A Note on Rayleigh's Criterion," *Combustion Science and Technology*, Vol. 56, 1987, pp. 159-166.
- ⁵Hartje, D. T., and Reardon, F. H., "Liquid Propellant Rocket Combustion Instability," NASA, Technical Rept. SP-194, 1972.
- ⁶Sirignano, W. A. a. C., L., "A Shock Wave Model of Unstable Rocket Combustion," *AIAA Journal*, Vol. Vol 2, No. No. 7, 1964.
- ⁷Zinn, B. T., "A Theoretical Study of Nonlinear Combustion Instability in Liquid Propellant Engines," *AIAA Journal*, Vol. 6, No. 10, 1968, pp. 1966-1972.
- ⁸Flandro, G. A., "Analysis of Nonlinear Combustion Instability," SIAM Minisymposium March 1998.
- ⁹Flandro, G. A., "Nonlinear Unsteady Solid Propellant Flame Zone Analysis," AIAA Paper 98-3700, 1998.
- ¹⁰Flandro, G. A., "Effects of Vorticity on Rocket Combustion Stability," *Journal of Propulsion and Power*, Vol. 11, No. 4, 1995, pp. 607-625.
- ¹¹Flandro, G. A., and Majdalani, J., "Aeroacoustic Instability in Rockets," *AIAA Journal*, Vol. 41, No. 3, 2003, pp. 485-497.
- ¹²Hartje, D. T. a. R., F. H., "Liquid Propellant Rocket Combustion Instability," NASA SP-194, 1972.
- ¹³Flandro, G. A., Majdalani, J., and French, J., "Incorporation of Nonlinear Capabilities in the Standard Stability Prediction Program," 40th AIAA Joint Propulsion Conference Paper AIAA 2004-4182, 2004.
- ¹⁴Flandro, G. A., Majdalani, J., and French, J., "Nonlinear Rocket Motor Stability Prediction: Limit Amplitude, Triggering, and Mean Pressure Shift," 40th AIAA Joint Propulsion Conference Paper AIAA 2004-4054, 2004.
- ¹⁵Sotter, J. G., Woodward, J. W., and Clayton, R. M., "Injector Response to Strong High-Frequency Pressure Oscillations," *Journal of Spacecraft & Rockets*, Vol. Vol. 6, No. No. 4, 1969, pp. 504-506.
- ¹⁶Sotter, J. G. a. C., R. M., "Monitoring the Combustion Process in Large Engines," *Journal of Spacecraft & Rockets*, Vol. Vol. 4, No. No. 5, 1967, pp. 702-703.
- ¹⁷Clayton, R. M., "Experimental Measurements on Rotating Detonation-Like Combustion," JPL, Technical Rept. 32-788, Pasadena, CA, August 1965.
- ¹⁸Clayton, R. M., Rogero, R. S., and Sotter, J. G., "An Experimental Description of Destructive Liquid Rocket Resonant Combustion," *AIAA Journal*, Vol. Vol 6, No. No. 7, 1968, pp. 1252-1259.
- ¹⁹Culick, F. E. C., "Combustion Instabilities in Propulsion Systems," *Unsteady Combustion*, Kluwer Academic Publishers, 1996, pp. 173-241.
- ²⁰Culick, F. E. C., "Stability of Three-Dimensional Motions in a Rocket Motor," *Combustion Science and Technology*, Vol. 10, No. 3, 1974, pp. 109-124.
- ²¹Culick, F. E. C., "The Stability of One-Dimensional Motions in a Rocket Motor," *Combustion Science and Technology*, Vol. 7, No. 4, 1973, pp. 165-175.
- ²²Culick, F. E. C., "Nonlinear Behavior of Acoustic Waves in Combustion Chambers," California Institute of Technology, Pasadena, CA, 1975.
- ²³Culick, F. E. C., and Yang, V., "Prediction of the Stability of Unsteady Motions in Solid Propellant Rocket Motors," *Nonsteady Burning and Combustion Stability of Solid Propellants*, Vol. 143, edited by L. De Luca, E. W. Price, and M. Summerfield, AIAA Progress in Astronautics and Aeronautics, Washington, DC, 1992, pp. 719-779.
- ²⁴Culick, F. E. C., "Acoustic Oscillations in Solid Propellant Rocket Chambers," *Acta Astronautica*, Vol. 12, No. 2, 1966, pp. 113-126.
- ²⁵Culick, F. E. C., "Rotational Axisymmetric Mean Flow and Damping of Acoustic Waves in a Solid Propellant Rocket," *AIAA Journal*, Vol. 4, No. 8, 1966, pp. 1462-1464.
- ²⁶Culick, F. E. C., "Stability of Longitudinal Oscillations with Pressure and Velocity Coupling in a Solid Propellant Rocket," *Combustion Science and Technology*, Vol. 2, No. 4, 1970, pp. 179-201.

- ²⁷Lovine, R. L., Dudley, D. P., and Waugh, R. D., "Standardized Stability Prediction Method for Solid Rocket Motors," Aerojet Solid Propulsion Co., Vols. I, II, III Rept. AFRPL TR 76-32, CA, May 1976.
- ²⁸Nickerson, G. R., Culick, F. E. C., and Dang, L. G., "Standardized Stability Prediction Method for Solid Rocket Motors Axial Mode Computer Program," Software and Engineering Associates, Inc., AFRPL TR-83-017, September 1983.
- ²⁹Flandro, G. A., "On Flow Turning," AIAA Paper 95-2530, July 1995.
- ³⁰Flandro, G. A., Cai, W., and Yang, V., "Turbulent Transport in Rocket Motor Unsteady Flowfield," *Solid Propellant Chemistry, Combustion, and Motor Interior Ballistics*, Vol. 185, edited by V. Yang, T. B. Brill, and W.-Z. Ren, AIAA Progress in Astronautics and Aeronautics, Washington, DC, 2000, pp. 837-858.
- ³¹Majdalani, J., Flandro, G. A., and Roh, T. S., "Convergence of Two Flowfield Models Predicting a Destabilizing Agent in Rocket Combustion," *Journal of Propulsion and Power*, Vol. 16, No. 3, 2000, pp. 492-497.
- ³²Majdalani, J., and Van Moorhem, W. K., "Improved Time-Dependent Flowfield Solution for Solid Rocket Motors," *AIAA Journal*, Vol. 36, No. 2, 1998, pp. 241-248.
- ³³Majdalani, J., "The Boundary Layer Structure in Cylindrical Rocket Motors," *AIAA Journal*, Vol. 37, No. 4, 1999, pp. 505-508.
- ³⁴Majdalani, J., "Vorticity Dynamics in Isobarically Closed Porous Channels. Part I: Standard Perturbations," *Journal of Propulsion and Power*, Vol. 17, No. 2, 2001, pp. 355-362.
- ³⁵Majdalani, J., and Roh, T. S., "Vorticity Dynamics in Isobarically Closed Porous Channels. Part II: Space-Reductive Perturbations," *Journal of Propulsion and Power*, Vol. 17, No. 2, 2001, pp. 363-370.
- ³⁶Majdalani, J., and Roh, T. S., "The Oscillatory Channel Flow with Large Wall Injection," *Proceedings of the Royal Society, Series A*, Vol. 456, No. 1999, 2000, pp. 1625-1657.
- ³⁷Vuillot, F., and Avalon, G., "Acoustic Boundary Layer in Large Solid Propellant Rocket Motors Using Navier-Stokes Equations," *Journal of Propulsion and Power*, Vol. 7, No. 2, 1991, pp. 231-239.
- ³⁸Roh, T. S., Tseng, I. S., and Yang, V., "Effects of Acoustic Oscillations on Flame Dynamics of Homogeneous Propellants in Rocket Motors," *Journal of Propulsion and Power*, Vol. 11, No. 4, 1995, pp. 640-650.
- ³⁹Yang, V., and Roh, T. S., "Transient Combustion Response of Solid Propellant to Acoustic Disturbance in Rocket Motors," AIAA Paper 95-0602, January 1995.
- ⁴⁰Vuillot, F., "Numerical Computation of Acoustic Boundary Layers in Large Solid Propellant Space Booster," AIAA Paper 91-0206, January 1991.
- ⁴¹Baum, J. D., Levine, J. N., and Lovine, R. L., "Pulsed Instabilities in Rocket Motors: A Comparison between Predictions and Experiments," *Journal of Propulsion Power*, Vol. 4, No. 4, 1988, pp. 308-316.
- ⁴²Baum, J. D., "Investigation of Flow Turning Phenomenon; Effects of Frequency and Blowing Rate," AIAA Paper 89-0297, January 1989.
- ⁴³Glick, R. L., and Renie, J. P., "On the Nonsteady Flowfield in Solid Rocket Motors," AIAA Paper 84-1475, June 1984.
- ⁴⁴Brown, R. S., Blackner, A. M., Willoughby, P. G., and Dunlap, R., "Coupling between Acoustic Velocity Oscillations and Solid Propellant Combustion," *Journal of Propulsion and Power*, Vol. 2, No. 5, 1986, pp. 428-437.
- ⁴⁵Shaeffer, C. W., and Brown, R. S., "Oscillatory Internal Flow Field Studies," United Technologies, AFOSR Contract Rept. F04620-90-C-0032, San Jose, CA 1990.
- ⁴⁶Shaeffer, C. W., and Brown, R. S., "Oscillatory Internal Flow Studies," United Technologies, Chemical Systems Div. Rept. 2060 FR, San Jose, CA, Aug. 1992.
- ⁴⁷Cantrell, R. H., and Hart, R. W., "Interaction between Sound and Flow in Acoustic Cavities: Mass, Momentum, and Energy Considerations," *Journal of the Acoustical Society of America*, Vol. 36, No. 4, 1964, pp. 697-706.
- ⁴⁸Brownlee, W. G., "Nonlinear Axial Combustion Instability in Solid Propellant Motors," *AIAA Journal*, Vol. 2, No. 2, 1964, pp. 275-284.
- ⁴⁹Flandro, G. A., "Approximate Analysis of Nonlinear Instability with Shock Waves," AIAA Paper 82-1220, July 1982.
- ⁵⁰Flandro, G. A., "Energy Balance Analysis of Nonlinear Combustion Instability," *Journal of Propulsion and Power*, Vol. 1, No. 3, 1985, pp. 210-221.
- ⁵¹Levine, J. N., and Baum, J. D., "A Numerical Study of Nonlinear Phenomena in Solid Rocket Motors," *AIAA Journal*, Vol. 21, No. 4, 1983, pp. 557-564.
- ⁵²Flandro, G. A., Majdalani, J., and Sims, J. D., "Nonlinear Longitudinal Mode Instability in Liquid Propellant Rocket Motor Preburner," *AIAA 2004-4162*, 2004.
- ⁵³Maslen, S. H. a. M., F. K., "On Strong Transverse Waves without Shocks in a Circular Cylinder," *Journal of the Aeronautical Sciences*, Vol. 23, 1956, pp. 583-593.
- ⁵⁴Oefelein, J. C., and Yang, V., "Comprehensive Review of Liquid-Propellant Combustion Instabilities in F-1 Engines," *Journal of Propulsion and Power*, Vol. 9, No. 5, 1993, pp. 657-677.

⁵⁵Flandro, G. A., and Sotter, J. G., "Unstable Combustion in Rockets," *Scientific American*, 1968.

⁵⁶Culick, F. E. C., Burnley, V. S., and Swenson, G., "Pulsed Instabilities in Solid-Propellant Rockets," *Journal of Propulsion Power*, Vol. 11, No. 4, 1995, pp. 657-665.

⁵⁷Culick, F. E. C., "Non-Linear Growth and Limiting Amplitude of Acoustic Oscillations in Combustion Chambers," *Combustion Science and Technology*, Vol. 3, No. 1, 1971, pp. 1-16.

⁵⁸Kirchoff, G., *Vorlesungen Über Mathematische Physik: Mechanik*, 2nd ed., Teubner, Leibzig, 1877, pp. 311-336.

⁵⁹Flandro, G. A., and Roach, R. L., "Effects of Vorticity Production on Acoustic Waves in a Solid Propellant Rocket," Air Force Office of Scientific Research, AFOSR Final Rept. 2060 FR, Bolling AFB, DC, Oct. 1992.

⁶⁰Malhotra, S., "On Combustion Instability in Solid Rocket Motors," Dissertation, California Institute of Technology, 2004.

⁶¹Van Moorhem, W. K., "An Investigation of the Origin of the Flow Turning Effect in Combustion Instability," 17th JANNAF Combustion Conference September 1980.

⁶²Blomshield, F. S., "Stability Testing and Pulsing of Full Scale Tactical Motors, Parts I and II," Naval Air Warfare Center, NAWCWPNS TP 8060, February, 1996 1996.